BMC Pulmonary Medicine

RESEARCH

Open Access

The presence of circulating genetically abnormal cells in blood predicts risk of lung cancer in individuals with indeterminate pulmonary nodules

Shahram Tahvilian[1], Joshua D. Kuban[2], David F. Yankelevitz[3], Daniel Leventon[1], Claudia I. Henschke[3], Jeffrey Zhu[3], Lara Baden[1], Rowena Yip[3], Fred R. Hirsch[4], Rebecca Reed[1], Ashley Brown[1], Allison Muldoon[1], Michael Trejo[1], Benjamin A. Katchman[1], Michael J. Donovan[1,5] and Paul C. Pagano[1*]

Abstract

Purpose Computed tomography is the standard method by which pulmonary nodules are detected. Greater than 40% of pulmonary biopsies are not lung cancer and therefore not necessary, suggesting that improved diagnostic tools are needed. The LungLB™ blood test was developed to aid the clinical assessment of indeterminate nodules suspicious for lung cancer. LungLB™ identifies circulating genetically abnormal cells (CGACs) that are present early in lung cancer pathogenesis.

Methods LungLB™ is a 4-color fluorescence *in-situ* hybridization assay for detecting CGACs from peripheral blood. A prospective correlational study was performed on 151 participants scheduled for a pulmonary nodule biopsy. Mann-Whitney, Fisher's Exact and Chi-Square tests were used to assess participant demographics and correlation of LungLB™ with biopsy results, and sensitivity and specificity were also evaluated.

Results Participants from Mount Sinai Hospital (n = 83) and MD Anderson (n = 68), scheduled for a pulmonary biopsy were enrolled to have a LungLB™ test. Additional clinical variables including smoking history, previous cancer, lesion size, and nodule appearance were also collected. LungLB™ achieved 77% sensitivity and 72% specificity with an AUC of 0.78 for predicting lung cancer in the associated needle biopsy. Multivariate analysis found that clinical and radiological factors commonly used in malignancy prediction models did not impact the test performance. High test performance was observed across all participant characteristics, including clinical categories where other tests perform poorly (Mayo Clinic Model, AUC = 0.52).

Conclusion Early clinical performance of the LungLB™ test supports a role in the discrimination of benign from malignant pulmonary nodules. Extended studies are underway.

Keywords Pulmonary nodules, Indeterminate nodules, Liquid biopsy, Lung cancer, Early detection

*Correspondence:
Paul C. Pagano
ppagano@lunglifeai.com

Full list of author information is available at the end of the article

© The Author(s) 2023. **Open Access** This article is licensed under a Creative Commons Attribution 4.0 International License, which permits use, sharing, adaptation, distribution and reproduction in any medium or format, as long as you give appropriate credit to the original author(s) and the source, provide a link to the Creative Commons licence, and indicate if changes were made. The images or other third party material in this article are included in the article's Creative Commons licence, unless indicated otherwise in a credit line to the material. If material is not included in the article's Creative Commons licence and your intended use is not permitted by statutory regulation or exceeds the permitted use, you will need to obtain permission directly from the copyright holder. To view a copy of this licence, visit http://creativecommons.org/licenses/by/4.0/. The Creative Commons Public Domain Dedication waiver (http://creativecommons.org/publicdomain/zero/1.0/) applies to the data made available in this article, unless otherwise stated in a credit line to the data.

Introduction

In 2022, the estimated number of new lung cancer cases in the United States is 236,740 with 130,180 deaths [1]. Identification of lung cancer at earlier stages results in more favorable prognoses and outcomes [2]. Lung cancer mortality has been slowly declining, mostly attributed to improved treatments and earlier diagnosis [1, 3]. Computed tomography (CT) was found to be capable of identifying lung cancers at an earlier, more curable stage [4], which was further supported by The National Lung Screening Trial (NLST) and Nederlands–Leuvens Longkanker Screenings Onderzoek (NELSON) studies that demonstrated a reduction in lung cancer-specific mortality when CT was used for screening in defined high-risk populations [5, 6]. Early-stage lung cancer continues to be challenging to detect due to low adherence to lung cancer screening guidelines and because early-stage disease is typically asymptomatic [1].

The majority of early-stage lung cancers are initially identified as indeterminate pulmonary nodules (IPNs), and an estimated 1.5 million IPNs are identified in the US each year using CT [7]. Guidelines, such as those from the American College of Chest Physicians (ACCP) and Fleischner Society are generally in alignment for low- or high-risk nodules, where the pre-test probability for lung cancer is <5% or >65%, respectively [8, 40]. For intermediate risk IPNs (5-65% pre-test probability for lung cancer), guidelines are poorly aligned and these nodules represent the most challenging to evaluate [9]. It is estimated that >40% of biopsies of CT-identified IPNs are negative for lung cancer [10], unnecessarily exposing individuals to invasive biopsy procedures, where approximately 20% of patients experience adverse events, including infection, pneumothorax, hemorrhage and even death from the procedure [10–12]. This highlights the need for an improved noninvasive method that provides additional information with higher confidence for individuals with IPNs.

Diagnosing cancer using blood has significant advantages: the process is minimally invasive and with very low risk of associated complications [11, 13]. Whole blood is a complex mixture that includes plasma and cell-based components, each of which contains unique biomarkers that can provide complementary information [14]. A main advantage of using blood compared with tissue biopsy is that the specimen is not restricted to a single tumor site, overcoming tumor heterogeneity and allowing more diverse sampling of circulating components from the tumor, such as circulating tumor cells (CTCs), circulating tumor DNA (ctDNA), and immune cells.

Laboratory and clinical investigations have revealed that lung epithelial cells have a reported capacity for motility thought to be derived from evolutionary requirements to repair damaged epithelium, as the need for motility-related wound healing likely preceded motility related to metastasis and carcinogenesis [15–17]. In lung cancer the early appearance of metastatic behavior has been demonstrated [17, 18]. Previous studies demonstrate that CTCs can be identified in patients with stage I lung cancer [18, 19], and those with chronic obstructive pulmonary disease (COPD) at high-risk for lung cancer years before a malignancy is observed radiographically [20]. Early metastatic behavior can be leveraged for early detection of lung cancer using various assays.

Numerous blood-based technologies have emerged to facilitate early detection of lung cancer by identifying RNA, proteins, circulating cell-free DNA (cfDNA), methylated cfDNA, ctDNA, or CTC [21–23]. These technologies are limited by their reliance on broad detection of molecular pathophysiological changes typically associated with high tumor burden in later-stage disease and are less likely to accurately detect early-stage lung cancer [21, 22]. Detection of ctDNA has had a marked impact on treatment stratification for late-stage lung cancer and this approach is being reevaluated for early-stage lung cancer. Low tumor cell burden limits the capacity to detect the smallest stage I lung cancers using existing ctDNA profiling methods [24]. Detecting early-stage lung cancer based on the presence of CTCs has been challenging given that CTCs are generally detected in small numbers in approximately 30% of patients with non-small cell lung cancer (NSCLC) [25–27]. Traditional CTC-based assays depend on the presence of epithelial markers to isolate and/or identify CTCs. Metastatic cancer cells commonly undergo epithelial to mesenchymal transition; identification of these CTCs is challenging using traditional approaches [29]. Due to the low sensitivity levels and suboptimal performance of these emerging technologies, they continue to be further optimized for clinical use [21, 30].

Chromosomal instability, a hallmark of cancer, can result in genomic copy number variations (CNVs) that can be readily detected with well-established technologies in individual cells, namely fluorescence in situ hybridization (FISH) [28]. FISH is employed by the LungLB™ test to detect CNVs in circulating genetically abnormal cells (CGACs) enriched from the peripheral blood of individuals with IPNs [28]. Studies have reported the presence of CGACs in individuals with various cancers, including lung cancer, and some of these CGACs have been identified as CTCs [28, 31, 32]. Individuals with cancer, including lung cancer, have been reported to have circulating lymphocytes with cytogenetic abnormalities that are identical to those found in cancerous cells from the primary tumor [28, 33–36]. As FISH is generally a highly specific assay for detecting chromosomal instability that is frequently observed in cancer, this method allows more comprehensive detection of multiple types

of CGACs that have been reported to be associated with lung cancer [28, 37].

Here we report the results of a study to assess clinical performance of the LungLB™ test, a liquid biopsy assay that utilizes immunomagnetic depletion combined with FISH, circumventing current cell marker restrictions of traditional CTC-based assays, to detect CGACs in individuals with IPNs. In this study, we evaluate concordance of lung nodule biopsy outcomes with the LungLB™ test results for participants with IPNs identified incidentally or through a lung cancer screening program.

Materials and methods

Participant enrollment

All participants meeting eligibility criteria and without preselection were enrolled from MD Anderson Cancer Center in Houston, Texas and the Mount Sinai Health System in New York, New York. Laboratory and statistical personnel were blinded to the results of the biopsy and clinical information. The results of the test did not direct or influence participant care. All sites had institutional review board approval, and informed written consent was obtained from all eligible participants.

Eligible participants were older than 18 years of age and scheduled for percutaneous needle biopsy. There were no restrictions on nodule characteristics. Participants were ineligible if they had a prior (3 year) or concurrent cancer diagnosis of any type, or a lung cancer diagnosis within the past 2 years. Inclusion and exclusion criteria were intentionally kept broad to avoid bias and reflect real-world conditions. This was an all-comers study and all eligible participants were enrolled on a "first-come, first-served" basis. Participants enrolled in this study were followed for 9–24 months following biopsy to confirm malignant or benign diagnosis using standard of care procedures at each site, including CT-based surveillance, repeat biopsy, and/or surgery.

Peripheral blood Collection

Peripheral blood was collected just prior to the CT-guided needle biopsy procedure. Blood was collected in vacutainer tubes containing blood stabilizer (Streck, Omaha, NE) and shipped overnight to LungLife AI's Clinical Laboratory Improvement Amendments (CLIA)-certified lab in Thousand Oaks, CA.

CGAC Enrichment and fluorescence *in situ* hybridization

A procedure and training set first describing the 4-probe FISH assay used by LungLB™ has been described previously [32]. Samples received by the CLIA-certified lab were accessioned using 2 unique identifiers. Blood was centrifuged at 1000 x g for 10 min with the brake off. Plasma was transferred to new tubes and stored at -80 °C. Erythrocytes were removed using an ammonium chloride-based erythrocyte lysis buffer. The remaining leukocytes were quantified using a BD Accuri™ C6 flow cytometer (Becton Dickenson, San Jose, CA) and 5,000,000 leukocytes were transferred to a new tube for magnetic cell depletion. We performed a depletion using the LungLB™ antibody cocktail to remove neutrophils and monocytes.

Ten thousand cells from the cell suspension were transferred to a glass slide using a cytospin instrument. Cells were fixed in Carnoy's fixative (3:1 solution of methanol and glacial acetic acid) for 30 minutes, followed by treatment with protease (pepsin pH 2, Abbot Molecular, Abbott Park, IL). Four colored FISH probes targeting chromosome locations 3q29 (Green), 3p22.1 (Red), 10p22.3 (Gold) and 10cen (Aqua), which localize to regions previously found to be altered in lung tumors [38], were then added to the microscope slide and a coverslip was affixed using rubber cement. DNA was denatured at 80 °C for 2 minutes, followed by overnight hybridization at 37 °C in a humidified chamber for 18 hours. Slides were washed to remove background in 72 °C wash buffer 1 (0.4x saline-sodium citrate (SSC) buffer/0.3% IGEPAL® CA-360, pH 7.0) for 1 minute followed by room temperature wash buffer 2 (2x SSC buffer/0.1% IGEPAL® CA-360, pH 7.0) for 1 minute. A new coverslip was applied with mounting medium containing 4',6-diamidino-2-phenylindole (DAPI; Vector Labs, Burlingame, CA) to visualize cell nuclei.

Image Acquisition and Analysis

Slides containing cells were imaged using a Bioview Allegro-Plus microscope system (Bioview USA, Billerica, MA). Images were acquired using a 60x objective (1.35 NA oil immersion on UPlanSapo, Olympus, Bartlett, TN) and a FLIR Grasshopper 3 monochrome camera (12-bit, 2448×2048 pixels, 3.4 µm pixel size, Edmund, Barrington, NJ) controlled using Bioview Duet software. All cells were imaged with 21 transverse sections spanning 0.65 µm.

Objects were classified by the Bioview Duet software according to probe copy number variation. Normal cells have 2 spots in all 4 color channels (Red, Green, Aqua, and Gold) and CGACs have a gain of spots in ≥2 color channels. Advanced CGACs were CGACs with the following specific anomalies: 4 spots in 2 color channels (4×2 Advanced CGAC), or a gain of spots in 2 color channels plus any loss of spots in 2 color channels (Double Deletion Advanced CGAC). Though Advanced CGACs can be considered a subtype of CGACs, classification of cells as a CGAC or Advanced CGAC was mutually exclusive in this study. Cells binned in the CGAC classes by the BioView Duet software were analyzed by a licensed technician who verified each cell. CGAC counts were normalized by dividing the CGAC count

by the total number of cells analyzed and multiplying by 10,000. A minimum of 10,000 cells were analyzed per participant. Total CGAC count, total cell count, and normalized CGAC counts were sent for unblinding for each participant.

Statistics

Statistical significance of clinical factor data was determined using the Mann–Whitney test (two-tailed, 95% confidence interval), Fisher's Exact test (two-tailed, 95% confidence interval), and Chi-Square test (two-tailed, 95% confidence interval). To determine the significance of different CGAC subtypes between participants with malignant and benign diagnosis, the Fisher's Exact Test (two-tailed, 95% confidence interval) or Chi-Square test (two-tailed, 95% confidence interval) were used depending on the sample size. A $P < .05$ was considered statistically significant in all analyses.

The nuclear area of cells was measured from DAPI stained cells using the Bioview software and data was exported to Prism (GraphPad Prism 9.3.0, San Diego, CA) for analysis of descriptive statistics.

To establish sensitivity, specificity, and area under the curve (AUC) for the LungLB™ test, we used the Youden Index to define a threshold of 2.47 CGAC cells per 10,000 cells. Receiver operating characteristic (ROC) analysis was performed in Prism using normalized CGAC counts from participants with malignant and benign nodules. For ROC analyses that were weighted for Advanced CGACs, the normalized CGAC ratio for samples containing Advanced CGACs was automatically set to 10.0 and declared qualitatively positive, regardless of the original CGAC ratio.

For the multivariate analysis, the predictors of interest (CGAC characteristic, age, gender, smoking status, COPD/Emphysema, subsolid/nonsolid nodule, nodule location, nodule size, and cancer history) were entered into a univariate and multivariate logistic regression model with cancer diagnosis as the outcome. The AUCs were compared using DeLong tests (two-sided). Complete case analysis was performed, and all analyses were completed in R v4.1.0 (R Foundation for Statistical Computing, Vienna, Austria).

Additional statistical analysis was performed to determine the calibration of the LungLB™ unweighted and weighted assay. Calibration curves were created by plotting predicted probabilities from the logistic regression model against the dichotomized diagnosis outcome and fitting the curve using the LOESS smoother. Brier score, Spiegelhalter scores and P values were calculated using the 'rms' package in R.

Results

Between December 2018 and February 2021, 182 participants were enrolled in the study; 19 participants were excluded from analysis, either due to an indeterminate biopsy result (n = 14) or having a sample that was unable to be processed due to clotting or damage (n = 5) (Figure S1). Samples from 12 of the 163 participants who met the initial eligibility criteria did not pass the assay quality control and these participants were excluded. A total of 151 participants met all study inclusion criteria. Of these 151 participants, 112 participants were diagnosed with malignant lung lesions and 39 participants with benign lung lesions based on blinded nodule biopsy results. Participant and disease characteristics commonly used in malignancy prediction models were compared in participants with benign versus malignant nodules and no statistically significant differences were found (Table 1). We also utilized the Mayo Clinic risk model to predict the probability of malignancy in this study cohort. With the Mayo Clinic Model, the majority of participants (107 [70.9%] of 151 participants) in our study fell into the intermediate-risk category as defined by ACCP guidelines (pre-test probability of malignancy between 5% and 65%), for which current management guidelines are not well-standardized and represents the most challenging diagnostic group.

CGAC characterization

The LungLB™ test utilizes a 4-color FISH assay to detect CNVs in cells from peripheral blood and identify CGACs. Figure 1a provides representative images of a normal white blood cell (WBC) with a diploid copy number per FISH probe, indicated by 2 spots detected per probe color channel (Red, Green, Aqua, and Gold). The LungLB™ test identifies CGACs based on a gain of spots in ≥2 color channels. Though there existed cells with spot abnormalities in a single-color channel, only cells with a gain in spots in ≥2 color channels were classified as CGACs. Examples of representative CGAC that were identified and used to differentiate benign from malignant participants are shown in Fig. 1b, c, and d. Advanced CGACs were detected in 44 (39.3%) samples from participants with confirmed malignant nodules vs. 4 (10.3%) samples from participants with confirmed benign nodules (Table 2). There was also a greater number of CGACs ($P = .004$) and Advanced CGACs ($P = .001$) identified among malignant versus benign participant samples.

To further characterize CGACs, we performed morphological analysis to compare nuclear area to the average nuclear area of each respective participant's normal WBCs. CGACs exhibited highly variable nuclear areas (range, 0.547x-2.776x relative to normal WBC), and we found that the mean nuclear area of Advanced CGACs

Table 1 Participant Characteristics (Negative for Lung Cancer, atypical cells, plural tumor, bronchiectasis)

Category, n (%)	Overall (N = 151)		*P* value
	Malignant Nodules (n = 112)	Benign Nodules (n = 39)	
Sample n/N, %	74.2	25.8	N/A
Gender			
Male	52 (46.4)	17 (43.6)	0.8525*
Female	60 (53.6)	22 (56.4)	
Age, Median (Range), y	70.0 (40.0)	71.0 (45.0)	0.7838†
Smoking Status			
Current	18 (16.1)	6 (15.4)	0.9115§
Former	70 (62.5)	26 (66.7)	
Never	23 (20.5)	7 (17.9)	
Unknown	1 (0.9)	0 (0)	
Median Pack Years, y	25.0	22.8	0.9083†
Nodule Location			
Upper Lobe	70 (62.5)	25 (64.1)	0.999
Non-upper lobe	42 (37.5)	14 (35.9)	
Nodule Size			
<1 cm	16 (14.3)	13 (33.3)	0.0654§
1 cm to <2 cm	41 (36.6)	13 (33.3)	
2 cm to <3 cm	32 (28.6)	7 (18.0)	
≥3 cm	23 (20.5)	6 (15.4)	
Malignant Lesion Type			
Adenocarcinoma	73 (65.2)	-	
Squamous Cell Carcinoma	17 (15.2)	-	
Small Cell and Neuroendocrine	17 (15.2)	-	
Other	5 (4.6)	-	
Cancer Stage			
I	76 (67.9)	-	
II	16 (14.2)	-	
III	7 (6.3)	-	
IV	8 (7.1)	-	
Unknown	5 (4.5)	-	
Benign Lesion Type			
Infectious Etiology	-	8 (20.5)	
Non-infectious Inflammation	-	5 (12.8)	
Hamartoma	-	3 (7.7)	
Scar	-	3 (7.7)	
Decrease in nodule size	-	4 (10.3)	
Other**	-	16 (41.0)	
Risk Stratification Based on Mayo Clinic Model			0.0883§
Low Risk (< 5%)	17 (15.2)	3 (7.7)	
Intermediate Risk (5-65%)	74 (66.1)	33 (84.6)	
High Risk (> 65%)	21 (18.7)	3 (7.7)	

* Fisher's Exact.

† Mann–Whitney.

§ Chi-square test.

**Other includes biopsy results of no malignant cells present, atypical cells, plural tumor, or bronchiectasis, which were followed between 9 and 24 months without diagnosis of malignancy.

was approximately 21.1% larger than the average WBC (95% CI, 13.6-28.6%) and approximately 13% larger than CGACs ($P<.0001$) (Figure S2 and Table S1).

LungLB™ Test Performance

We evaluated the overall performance and diagnostic efficacy of the LungLB™ test by plotting ROC curves in comparison with the ROC from the Mayo Clinic Model and positron emission tomography (PET) scan results. The Mayo Clinic Model was chosen as a comparator because it is the most frequently used probability model and was developed using the general population, rather than an isolated cohort, reflecting the population for which LungLB™ is intended to be offered [39]. ROC analysis of the full data set consisting of 151 participants revealed an AUC of 0.74 (95% CI, 0.66–0.84; $P<.001$) with 67.9% sensitivity and 74.4% specificity, compared with an AUC of 0.52 using the Mayo Clinic Model and an AUC of 0.57 using the PET imaging results available (Fig. 2A; Table 3). We observed that Advanced CGACs were more highly associated with malignant lung cancer diagnosis, and an additional ROC analysis where Advanced CGACs were weighted more heavily revealed an AUC of 0.78 (95% CI, 0.70–0.87; $P<.0001$) with 77% sensitivity and 72% specificity, compared with an AUC of 0.52 using the Mayo Clinic Model and an AUC of 0.57 using the PET imaging results available (Fig. 2B; Table 3). To ensure that our LungLB™ assay is in calibration we plotted a calibration curve using both the unweighted and weighted assays (Figure S3). For each calibration plot, the Brier score was calculated to determine fit, where a score closer to 0 represents a good fit (0.163 [unweighted] and 0.158 [weighted]). Using the Brier score and Spiegelhalter z-score we calculated a Spiegelhalter p-value to test for misclassification. A $P<.05$ would indicate our model is poorly calibrated. LungLB™ assay has a P value of 0.88 (unweighted) and 0.81 (weighted) indicating that the LungLB™ assay is calibrated properly.

Diagnostic efficacy of the LungLB™ test was also evaluated for various participant characteristics, including nodule size and consistency, lung cancer subtype and stage, and smoking history (Table 3). The LungLB™ test demonstrated robust performance for each participant characteristic category. Superior LungLB™ test performance was observed with nodules <2 cm in size (AUC = 0.83) vs. ≥2 cm in size (AUC = 0.70), sub/nonsolid nodules (AUC = 0.90) vs. solid nodules (AUC = 0.72) and may be better in stage I (AUC = 0.80) vs. stage II-IV disease (AUC = 0.67). Comparable test performance was observed between lung cancer subtypes (adenocarcinoma, AUC = 0.79; squamous cell carcinoma, AUC = 0.83; and small cell and neuroendocrine, AUC = 0.75) and smoking history (Ever, AUC = 0.79; and Never, AUC = 0.81).

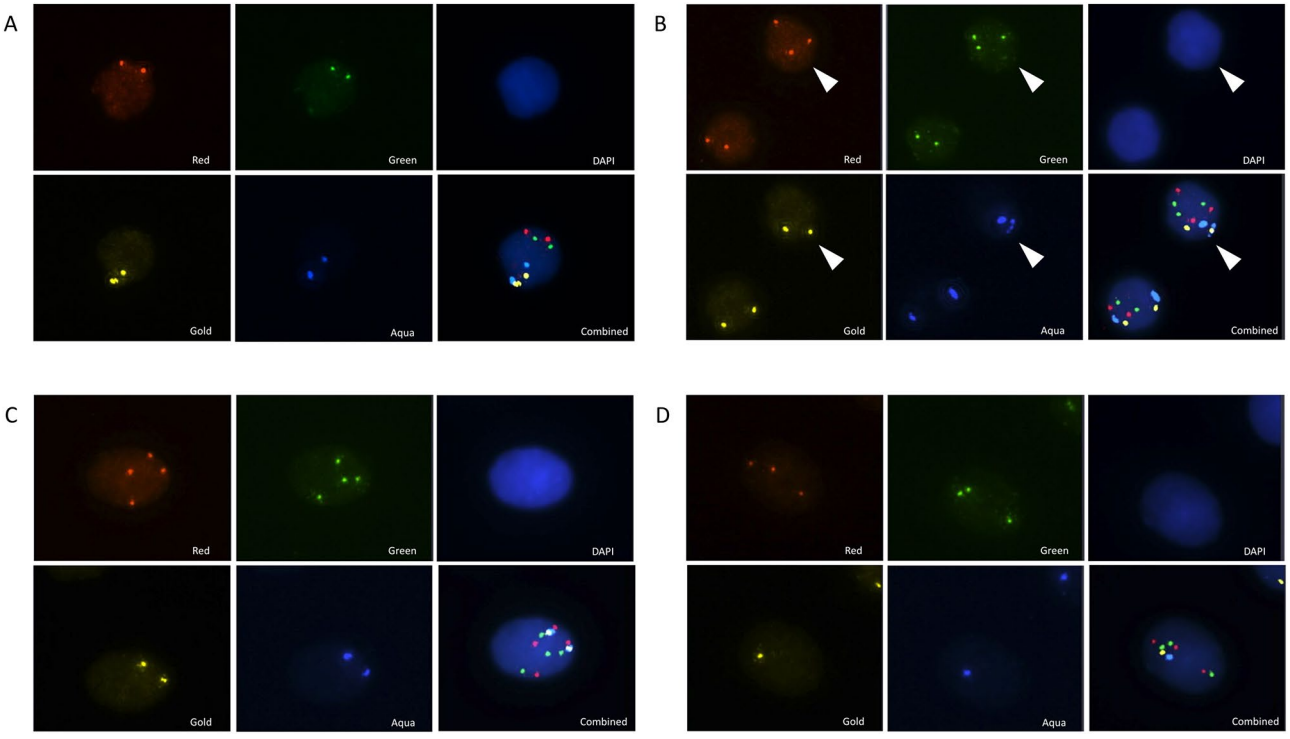

Fig. 1 Representative fluorescence microscopy images from the LungLB™ test demonstrating (A) a normal WBC with 2 spots in the Red (3p22.1), Green (3q29), Aqua (10cen), and Gold (10q22.3) color channels, (B) a CGAC, indicated by the white arrow, with an extra spot in the Red and Green channels, (C) an Advanced CGAC with 4 spots each in the Red and Green channels (4×2 Advanced CGAC), and (D) an Advanced CGAC with an extra spot in the Red and Green channels and a spot loss in the Gold and Aqua channels (Double Deletion Advanced CGAC). Cell nuclei are visualized in the DAPI channel. Abbreviations: CGAC, circulating genetically abnormal cell; DAPI, 4′,6-diamidino-2-phenylindole; WBC, white blood cell.

Table 2 CGAC and Advanced CGAC Cell Counts in Malignant and Benign Participant Samples

n (%)	Total Participant Samples (n = 151)	Malignant Participant Samples (n = 112)	Benign Participant Samples (n = 39)	*P* value (Malignant vs. Benign Participant Samples)
Advanced CGAC	48 (31.8)	44 (39.3)	4 (10.3)	0.001*

Abbreviations: CGAC, circulating genetically abnormal cell

* Chi-Square Test

To evaluate the independent and associated contribution of readily available clinical factors (e.g., age, sex, smoking history, presence of COPD/emphysema, nodule type, location and size, and cancer history) we performed a stepwise multivariable analysis (Table S2). CGAC were the strongest independent predictor of malignancy in this study. Although there were no statistically significant differences when we compared the AUCs across the different models when combining CGAC with clinical factors, comparison of Model 3 (Clinical Factors) vs. Model 5 (Clinical Factors + Weighted CGAC Ratio) revealed a $P = .053$, which suggests that combining CGAC to clinical factors may improve the diagnostic efficacy of the LungLB™ test compared with when clinical factors are used alone (Table S3).

To describe how LungLB™ may be useful clinically, we describe three example cases in Table 4 and how LungLB™ may have saved critical time in determining a final treatment regimen. In each of the three cases the Mayo Risk Score (pretest probability) fell into or near the intermediate risk category (25%, 67%, and 47%), representing challenging cases to evaluate. All three cases had a negative or indeterminate biopsy result. LungLB™ results indicated an increased risk for malignancy for all three cases. Following the initial biopsy Cases 1 and 2 underwent imaging-based follow-up, followed by surgical treatment and final diagnosis of Stage I Adenocarcinoma and Stage IA3 Adenocarcinoma, respectively. Case 3 underwent a follow-up biopsy in May 2020 on the lymph nodes, in which one tested positive for small cell lung cancer.

Discussion

For individuals with IPNs, various clinical and radiologic factors have been found to be associated with higher risk of lung cancer [9]. The Mayo Clinic developed a highly

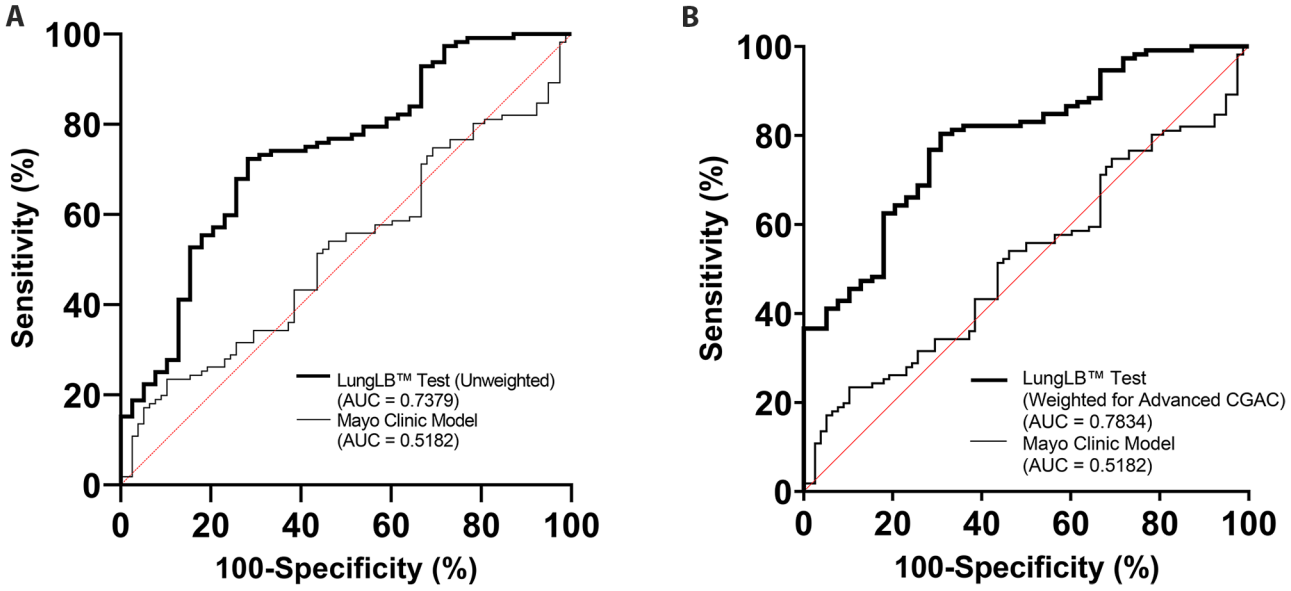

Fig. 2 ROC analysis of (A) the LungLB™ test without weighting of Advanced CGACs (AUC = 0.74) and (B) the LungLB™ test with weighting of Advanced CGACs (AUC = 0.78) compared with the Mayo Model (AUC = 0.52). Abbreviations: AUC, area under the curve.

Table 3 LungLB™ Test Performance by Participant Characteristic

Category	n	AUC	Sensitivity (%)	Specificity (%)
All Samples (Mayo Clinic Model)	151	0.5182	23.4	89.7
Samples with Available PET Scan	79	0.5674	67.2	.4
All Samples (Unweighted)	151	0.7379	67.9	74.4
All Samples (Weighted for Advanced CGACs)	151	0.7834	76.8	71.8
Nodule Size				
< 2 cm	83	0.8269	83.9	69.5
≥ 2 cm	68	0.7049	69.1	69.2
Nodule Consistency				
Solid	92	0.7215	65.2	65.2
Subsolid	41	0.8952	83.3	80.0
Cancer Stage				
I	76	0.7945	79.0	74.4
II-IV	31	0.6716	61.3	71.8
Unknown	5	0.7333	80.0	71.8
Malignant Lesion Type				
Adenocarcinoma	73	0.7875	72.6	74.4
Squamous Cell Carcinoma	17	0.8250	88.2	71.8
Small Cell and Neuroendocrine	17	0.7541	76.5	71.8
Other	5	0.6970	60.0	69.2
Smoking History				
Ever	120	0.7929	76.4	71.0
Never	30	0.8075	78.3	85.7

Abbreviations: AUC, area under the curve, CGAC, circulating genetically abnormal cell, PET, positron emission tomography. Results from all 39 benign nodules were used as the comparator for cancer stage and malignant lesion type

validated and commonly used model that relies on an individual's age, smoking status, history of cancer, and nodule characteristics to predict lung cancer risk in individuals with suspicious lung lesions [40, 41]. Assessment of these factors alone has proved insufficient for high confidence risk stratification of individuals with IPNs and there exists a need for additional independent predictors and biomarkers of lung cancer [9]. We applied the Mayo Clinic Model to characterize the participants in our study, as it is the most validated risk model [40, 41], and 15.9% of participants had high and 13.2% had low pre-test probability of lung cancer. The majority (70.9%) of participants fell into the intermediate-risk class, for which risk stratification in clinical practice remains challenging [9, 40]. Notably, the Mayo model performed poorly in our study. This is because the factors used in the Mayo model were indistinguishable between benign and malignant nodules in our study population, which is similar to the DECAMP study population described by Kammer et al. [42], where the AUC for the Mayo Model was 0.59. However, this population would derive the greatest benefit from improved lung cancer prediction tests evaluating novel biomarkers, such as the LungLB™ test, that can better inform clinical decision-making.

To evaluate the performance of the LungLB™ test, multivariate analysis revealed that CGACs were the strongest independent predictor of malignant lung cancer and improved predictive power was achieved when used in adjunct with clinical factors. This finding suggests that CGACs may serve as a useful biomarker, and integrating CGAC count with clinical factors in lung cancer risk assessments may provide superior results with greater

Table 4 Example Case Studies

Case	Mayo Risk Score	Initial CT/ Nodule Size	Biopsy Date/ Result	LungLB™ Date/ Result	Surgery Date/ Result	Days LungLB™ may have saved
1	25%	Nov 2018/ 1.3 cm	Jan 2020/ Negative	Jan 2020/ 6.97	Jan 2021/ Stage 1 Adenocarcinoma	365
2	67%	July 2019/ 2.6 cm	Aug 2019/ Indeterminate	Aug 2019/ 11.89	Sept 2021/ Stage IA3 Adenocarcinoma	517
3	47%	Oct 2019/ 1.68 cm	Mar 2020/ Atypical-rare atypical cells	Mar 2020/ 2.85	May 2020/ N2 & N3 Small Cell Lung Cancer	60

Abbreviations: CT, computerized tomography scan

confidence, although more work needs to be done to verify this [9]. In addition to risk models, guidelines recommend the use of fluorodeoxyglucose PET for indeterminate nodule evaluation in certain situations. PET utility has been called into question, especially for nodules <2 cm and in areas of endemic granulomatous disease [43]. In our study, 52% of study participants had PET scan performed, and based on the commonly accepted cut-off of SUV_{max}=2.5 [44], PET performed with 67.2% sensitivity and 44.4% specificity (AUC=0.56). Further investigation and additional studies showing the clinical utility of LungLB™ would strengthen our understanding of its value.

The diagnostic value of Advanced CGACs was found to be greater than other CGACs in detecting malignant lung cancer. We discovered that Advanced CGACs displayed a larger average nuclear area compared with normal WBCs and other CGACs. Abnormal nuclear morphologies, including an enlarged nucleus, have been previously reported in malignant cells, which support our finding that Advanced CGACs are more highly correlated with malignancy in the LungLB™ test [45–47].

This discovery has additional implications for other diagnostic tests that detect CTCs. CTC enrichment commonly relies on isolation based on cell surface markers and size exclusion [48–51]. Therefore, CGACs without expression of traditional CTC surface markers or that fall outside of the isolation size window would be excluded in these tests. The LungLB™ test utilizes FISH to identify CGACs, which allows for more unbiased detection of CGACs regardless of their surface marker expression profile or size.

Our analyses revealed that the LungLB™ test displayed consistent and robust performance across various participant characteristics. The LungLB™ test continued to display robust performance even in participants with smaller (<2 cm) nodules, sub/nonsolid nodules, and stage I disease, although the small number of participants with stage II-IV disease in this study warrants further investigation. Our finding that the LungLB™ test performed well in participants with stage I disease was surprising, given that other cancer detection tests typically exhibit poor performance with detecting early-stage disease [22, 30]. The LungLB™ test demonstrated 79.0% sensitivity in stage I lung cancer and 61.3% sensitivity across stage II-IV lung cancer. This finding is particularly impactful given that early-stage lung cancer is where there currently exists the greatest unmet need in terms of an accurate, minimally invasive diagnostic test. We propose that the higher performance associated particularly with subsolid, smaller-sized, earlier-stage malignant lesions may be related to their disease pathogenesis. Lung cancer has been shown to exhibit early metastatic behavior both clinically and in pre-clinical models of cells representative of premalignant lesions [17], which often manifest as subsolid lesions by CT. With tumor progression, fast growing cells in a tumor may outpace highly motile, slow-growing cells as the dominant cell type as described due to a "Grow or Go" phenotypic switch [52, 53], which may result in altered tumor-associated cells, such as CGAC, in circulation.

The majority of participants with malignant lesions had adenocarcinoma (>65%); the low number of participants with squamous cell carcinoma and small cell/neuroendocrine carcinomas make it challenging to accurately assess test performance by lung cancer subtype. Future studies with expanded patient numbers are underway to further refine our understanding of performance in these subtypes.

The LungLB™ test also may offer earlier detection of lung cancer compared with current standard of care as well as sparing individuals from unnecessary biopsies (Table 3, stage I detection with 79.0% sensitivity and 74.4% specificity). In the described cases, initial biopsies indicated a negative or indeterminate diagnosis. Meanwhile, the LungLB™ test, which was performed concurrently with the biopsies, positively indicated lung cancer in each case. Later analysis of surgically resected tissue revealed that each patient had lung cancer. Notably in Case 2, surgical resection of the nodule did not occur until 2 years after the initial biopsy, which may have been due to COVID-related disruptions in care. Had LungLB™

been used in the nodule evaluation process, each of these patients may have received treatment months to years earlier than with the current diagnostic pathway. Although the volume doubling times of IPNs are highly variable, malignant lung cancer nodules are associated with rapid doubling times and aggressive metastasis; therefore, delays in proper diagnosis and treatment of malignant lung cancer have significant implications and may lead to poorer patient outcomes [54]. The inability to provide accurate diagnoses with initial biopsies also subjects patients to the burden of frequent follow-up screenings and examinations and continued anxiety, especially if the biopsy procedure resulted in an adverse event. This highlights the broad potential clinical utility of the LungLB™ test.

This study is not without limitations. All participant samples were collected from 2 sites and comprise a relatively limited sample set, which does not span the full diversity of patient demographics nor IPNs that exist. The follow-up range was broad (9–24 months), and while most participants had received a diagnosis within months, there were a minority of cases where diagnostic delays were COVID-related. Our multivariate analysis was performed to identify independent predictors of malignancy in this dataset; we do not propose it be used as a clinical model for nodule evaluation as this would require a separate validation. These models were developed using a small dataset and therefore there is risk of overfitting. Of importance to note is that one of the sites we enrolled participants was MD Anderson Cancer Center in Houston, Texas, which is in a region with higher incidence of fungal histoplasmosis infections. For clinicians, distinguishing infectious etiology from lung cancer is often challenging and presence of histoplasmosis infection can confound lung cancer diagnosis [43]. In our study, 11 (28.2%) of 39 participants with benign lesions had infectious etiology. The LungLB™ test maintained strong performance in these individuals with confounding lung infections, further demonstrating its promise in diagnosing lung cancer in challenging populations.

The LungLB™ test utilizes FISH, a highly specific and sensitive assay, to detect DNA CNVs that are a hallmark of cancer to broadly detect CGACs. However, because the test does not rely on the traditional markers of CTCs to identify CGACs, further characterization of CGACs is warranted and immunophenotyping of these cell populations is underway. Further characterization of these cells may help in understanding the pathogenesis of lung cancer, as well as provide the potential for identification of additional cell markers that may be used to further improve the performance of the LungLB™ test. Additionally, novel biomarker targets may also be revealed, which may be leveraged in the development of targeted therapies.

Our data indicate that the LungLB™ test, a minimally invasive liquid biopsy, FISH-based assay, may discriminate benign from malignant processes in individuals with IPNs at risk for lung cancer. We report that the LungLB™ test performs with high specificity and sensitivity, which may be further enhanced when combined with clinical factors. Additional studies of the LungLB™ test are warranted.

Abbreviations

CGACs	Circulating Genetically Abnormal Cells
CT	Computed Tomography
IPNs	Indeterminate Pulmonary Nodules
CTC	Circulating Tumor Cells
COPD	Chronic Obstructive Pulmonary Disease
ctDNA	Circulating Tumor DNA
cfDNA	Cell Free DNA
NSCLC	Non-Small Cell Lung Cancer
CNV	Copy Number Variation
FISH	Fluorescence *in situ* Hybridization
AUC	Area Under the Curve
ROC	Receiver Operating Characteristic
WBC	White Blood Cells
PET	Positron Emission Tomography

Supplementary Information

The online version contains supplementary material available at https://doi.org/10.1186/s12890-023-02433-4.

Supplementary Material 1

Supplementary Material 2

Supplementary Material 3

Supplementary Material 4

Supplementary Material 5

Supplementary Material 6

Acknowledgements

This study was sponsored by LungLife AI. The authors thank the investigators and participants who volunteered in this study. Stephanie Weng, PhD provided medical writing support, which was funded by LungLife AI. We thank Lucia Chen, PhD for providing statistical support, which was funded by LungLife AI.

Author Contribution

ST, LB, PCP, CIH, and JDK conceived and designed the study. ST, DL, LB, RR, AB, AM, and MT performed all the laboratory work and analyzed results. ST, BAK, and PCP implemented the analysis and prepared the figures. JDK, DFY, CIH, JZ, RY, FRH, and MJD enrolled participants, collected samples and provided clinical results. BAK and PCP drafted and revised the manuscript. All authors have read and approved the final manuscript.

Funding

Funding for the study was provided by LungLifeAI, Inc. LungLifeAI, Inc. drafted the study, oversaw the analysis and manuscript preparation, and approved the decision to publish.

Data Availability

The datasets generated during the current study are not publicly available due to concerns regarding participant confidentiality and proprietary information but are available upon reasonable request from the corresponding author.

Declarations

Ethics approval and consent to participate
This study was a multi-center prospective study that included patients with lung nodules identified through CT either through a screening program or incidental finding at participating medical centers in the U.S. Ethics review and approval was obtained by each institution before enrollment and written informed consent was obtained from all patients. All methods were carried out in accordance with relevant guidelines and regulations or declarations of Helsinki.
The site name, corresponding ethics committee/Institutional Review Board (IRB), and the IRB number for each site participating in the study is shown below.

Consent for Publication
Not applicable.

Competing Interests
JDK, DFY, CUH, JZ, RY, FRH, and MJD receive sponsored research funding from LungLife AI. ST, LB, DL, RR, AB, AM, MT, BAK, and PCP are employees of LungLife AI.

Author details
[1]LungLife AI, Inc, 2545 W. Hillcrest Drive, Suite 140, Thousand Oaks, CA, USA
[2]Department of Interventional Radiology, The University of Texas MD Anderson Cancer Center, Houston, TX, USA
[3]Department of Radiology, Icahn School of Medicine at Mount Sinai, New York, NY, USA
[4]Icahn School of Medicine, Center for Thoracic Oncology, Tisch Cancer Institute at Mount Sinai, New York, NY, USA
[5]Department of Pathology, Cancer Institute, Icahn School of Medicine at Mount Sinai, New York, NY, USA

Received: 7 February 2023 / Accepted: 13 April 2023
Published online: 05 June 2023

References

1. Siegel RL, Miller KD, Fuchs HE, Jemal A. Cancer Statistics, 2021. CA Cancer J Clin. 2021;71(1):7–33.
2. Knight SB, Crosbie PA, Balata H, Chudziak J, Hussell T, Dive C. Progress and prospects of early detection in lung cancer. Open Biol. 2017;7(9):170070.
3. Flores R, Patel P, Alpert N, Pyenson B, Taioli E. Association of Stage Shift and Population Mortality among patients with Non-Small Cell Lung Cancer. JAMA Netw Open. 2021;4(12):e2137508.
4. Henschke CI, McCauley DI, Yankelevitz DF, Naidich DP, McGuinness G, Miettinen OS, Libby DM, Pasmantier MW, Koizumi J, Altorki NK, et al. Early Lung Cancer Action Project: overall design and findings from baseline screening. Lancet. 1999;354(9173):99–105.
5. National Lung Screening Trial, Research T, Aberle DR, Adams AM, Berg CD, Black WC, Clapp JD, Fagerstrom RM, Gareen IF, Gatsonis C, Marcus PM, et al. Reduced lung-cancer mortality with low-dose computed tomographic screening. N Engl J Med. 2011;365(5):395–409.
6. de Koning HJ, van der Aalst CM, de Jong PA, Scholten ET, Nackaerts K, Heuvelmans MA, Lammers JJ, Weenink C, Yousaf-Khan U, Horeweg N, et al. Reduced lung-Cancer mortality with volume CT screening in a Randomized Trial. N Engl J Med. 2020;382(6):503–13.
7. Gould MK, Tang T, Liu IL, Lee J, Zheng C, Danforth KN, Kosco AE, Di Fiore JL, Suh DE. Recent Trends in the identification of Incidental Pulmonary Nodules. Am J Respir Crit Care Med. 2015;192(10):1208–14.
8. Bueno J, Landeras L, Chung JH. Updated Fleischner Society Guidelines for managing Incidental Pulmonary Nodules: common questions and challenging scenarios. Radiographics. 2018;38(5):1337–50.
9. Paez R, Kammer MN, Massion P. Risk stratification of indeterminate pulmonary nodules. Curr Opin Pulm Med. 2021;27(4):240–8.
10. Lokhandwala T, Bittoni MA, Dann RA, D'Souza AO, Johnson M, Nagy RJ, Lanman RB, Merritt RE, Carbone DP. Costs of Diagnostic Assessment for Lung Cancer: a Medicare Claims Analysis. Clin Lung Cancer. 2017;18(1):e27–e34.
11. Huo J, Xu Y, Sheu T, Volk RJ, Shih YT. Complication rates and downstream medical costs Associated with Invasive Diagnostic Procedures for Lung Abnormalities in the community setting. JAMA Intern Med. 2019;179(3):324–32.
12. Handy JR Jr, Skokan M, Rauch E, Zinck S, Sanborn RE, Kotova S, Wang M. Results of Lung Cancer Screening in the community. Ann Fam Med. 2020;18(3):243–9.
13. Zugazagoitia J, Ramos I, Trigo JM, Palka M, Gomez-Rueda A, Jantus-Lewintre E, Camps C, Isla D, Iranzo P, Ponce-Aix S, et al. Clinical utility of plasma-based digital next-generation sequencing in patients with advance-stage lung adenocarcinomas with insufficient tumor samples for tissue genotyping. Ann Oncol. 2019;30(2):290–6.
14. Hodara E, Morrison G, Cunha A, Zainfeld D, Xu T, Xu Y, Dempsey PW, Pagano PC, Bischoff F, Khurana A, et al. Multiparametric liquid biopsy analysis in metastatic prostate cancer. JCI Insight. 2019;4(5):e125529.
15. Vaughan AE, Brumwell AN, Xi Y, Gotts JE, Brownfield DG, Treutlein B, Tan K, Tan V, Liu FC, Looney MR, et al. Lineage-negative progenitors mobilize to regenerate lung epithelium after major injury. Nature. 2015;517(7536):621–5.
16. Kathiriya JJ, Brumwell AN, Jackson JR, Tang X, Chapman HA. Distinct airway epithelial stem cells hide among Club cells but mobilize to promote alveolar regeneration. Cell Stem Cell. 2020;26(3):346–58.
17. Pagano PC, Tran LM, Bendris N, O'Byrne S, Tse HT, Sharma S, Hoech JW, Park SJ, Liclican EL, Jing Z, et al. Identification of a human airway epithelial cell subpopulation with altered Biophysical, Molecular, and Metastatic Properties. Cancer Prev Res (Phila). 2017;10(9):514–24.
18. Tanaka F, Yoneda K, Kondo N, Hashimoto M, Takuwa T, Matsumoto S, Okumura Y, Rahman S, Tsubota N, Tsujimura T, et al. Circulating tumor cell as a diagnostic marker in primary lung cancer. Clin Cancer Res. 2009;15(22):6980–6.
19. Chemi F, Rothwell DG, McGranahan N, Gulati S, Abbosh C, Pearce SP, Zhou C, Wilson GA, Jamal-Hanjani M, Birkbak N, et al. Pulmonary venous circulating tumor cell dissemination before tumor resection and disease relapse. Nat Med. 2019;25(10):1534–9.
20. Ilie M, Hofman V, Long-Mira E, Selva E, Vignaud JM, Padovani B, Mouroux J, Marquette CH, Hofman P. Sentinel" circulating tumor cells allow early diagnosis of lung cancer in patients with chronic obstructive pulmonary disease. PLoS ONE. 2014;9(10):e111597.
21. Seijo LM, Peled N, Ajona D, Boeri M, Field JK, Sozzi G, Pio R, Zulueta JJ, Spira A, Massion PP, et al. Biomarkers in Lung Cancer Screening: achievements, promises, and Challenges. J Thorac Oncol. 2019;14(3):343–57.
22. Freitas C, Sousa C, Machado F, Serino M, Santos V, Cruz-Martins N, Teixeira A, Cunha A, Pereira T, Oliveira HP, et al. The role of Liquid Biopsy in early diagnosis of Lung Cancer. Front Oncol. 2021;11:634316.
23. Xing W, Sun H, Yan C, Zhao C, Wang D, Li M, Ma J. A prediction model based on DNA methylation biomarkers and radiological characteristics for identifying malignant from benign pulmonary nodules. BMC Cancer. 2021;21(1):263.
24. Abbosh C, Birkbak NJ, Swanton C. Early stage NSCLC - challenges to implementing ctDNA-based screening and MRD detection. Nat Rev Clin Oncol. 2018;15(9):577–86.
25. de Wit S, van Dalum G, Lenferink AT, Tibbe AG, Hiltermann TJ, Groen HJ, van Rijn CJ, Terstappen LW. The detection of EpCAM(+) and EpCAM(-) circulating tumor cells. Sci Rep. 2015;5:12270.
26. de Wit S, Rossi E, Weber S, Tamminga M, Manicone M, Swennenhuis JF, Groothuis-Oudshoorn CGM, Vidotto R, Facchinetti A, Zeune LL, et al. Single tube liquid biopsy for advanced non-small cell lung cancer. Int J Cancer. 2019;144(12):3127–37.
27. Tamminga M, Andree KC, Hiltermann TJN, Jayat M, Schuuring E, van den Bos H, Spierings DCJ, Lansdorp PM, Timens W, Terstappen L et al. Detection of Circulating Tumor Cells in the Diagnostic Leukapheresis Product of Non-Small-Cell Lung Cancer Patients Comparing CellSearch((R)) and ISET. Cancers (Basel) 2020, 12(4).
28. Katz RL, He W, Khanna A, Fernandez RL, Zaidi TM, Krebs M, Caraway NP, Zhang HZ, Jiang F, Spitz MR, et al. Genetically abnormal circulating cells in lung cancer patients: an antigen-independent fluorescence in situ hybridization-based case-control study. Clin Cancer Res. 2010;16(15):3976–87.
29. Chaffer CL, Weinberg RA. A perspective on cancer cell metastasis. Science. 2011;331(6024):1559–64.
30. Klein EA, Richards D, Cohn A, Tummala M, Lapham R, Cosgrove D, Chung G, Clement J, Gao J, Hunkapiller N, et al. Clinical validation of a targeted methylation-based multi-cancer early detection test using an independent validation set. Ann Oncol. 2021;32(9):1167–77.

31. Feng M, Lin M, Zhou H, Zhu Y, Chen B, Ye X, Huang C, Zhang J, Bai C. Clinical utility of circulating genetically abnormal cells within low-dose computed tomography lung cancer screening: a correlative MCPND trial study. J Clin Oncol. 2020;38(15suppl):e15536–6.
32. Katz RL, Zaidi TM, Pujara D, Shanbhag ND, Truong D, Patil S, Mehran RJ, El-Zein RA, Shete SS, Kuban JD. Identification of circulating tumor cells using 4-color fluorescence in situ hybridization: validation of a noninvasive aid for ruling out lung cancer in patients with low-dose computed tomography-detected lung nodules. Cancer Cytopathol. 2020;128(8):553–62.
33. Rossner P, Boffetta P, Ceppi M, Bonassi S, Smerhovsky Z, Landa K, Juzova D, Sram RJ. Chromosomal aberrations in lymphocytes of healthy subjects and risk of cancer. Environ Health Perspect. 2005;113(5):517–20.
34. Wang H, Wang Y, Kota KK, Sun B, Kallakury B, Mikhail NN, Sayed D, Mokhtar A, Maximous D, Yassin EH, et al. Strong associations between chromosomal aberrations in blood lymphocytes and the risk of urothelial and squamous cell carcinoma of the bladder. Sci Rep. 2017;7(1):13493.
35. Dave BJ, Hopwood VL, King TM, Jiang H, Spitz MR, Pathak S. Genetic susceptibility to lung cancer as determined by lymphocytic chromosome analysis. Cancer Epidemiol Biomarkers Prev. 1995;4(7):743–9.
36. Zhu Y, Spitz MR, Strom S, Tomlinson GE, Amos CI, Minna JD, Wu X. A case-control analysis of lymphocytic chromosome 9 aberrations in lung cancer. Int J Cancer. 2002;102(5):536–40.
37. Ye M, Zheng X, Ye X, Zhang J, Huang C, Liu Z, Huang M, Fan X, Chen Y, Xiao B, et al. Circulating genetically abnormal cells add non-invasive diagnosis value to Discriminate Lung Cancer in patients with Pulmonary Nodules =10 mm</at. Front Oncol. 2021;11:638223.
38. Yendamuri S, Vaporciyan AA, Zaidi T, Feng L, Fernandez R, Bekele NB, Hofstetter WL, Jiang F, Mehran RJ, Rice DC, et al. 3p22.1 and 10q22.3 deletions detected by fluorescence in situ hybridization (FISH): a potential new tool for early detection of non-small cell lung Cancer (NSCLC). J Thorac Oncol. 2008;3(9):979–84.
39. Choi HK, Ghobrial M, Mazzone PJ. Models to Estimate the Probability of Malignancy in patients with pulmonary nodules. Ann Am Thorac Soc. 2018;15(10):1117–26.
40. Gould MK, Donington J, Lynch WR, Mazzone PJ, Midthun DE, Naidich DP, Wiener RS. Evaluation of individuals with pulmonary nodules: when is it lung cancer? Diagnosis and management of lung cancer, 3rd ed: american college of chest Physicians evidence-based clinical practice guidelines. Chest. 2013;143(5 Suppl):e93S–e120S.
41. Yang B, Jhun BW, Shin SH, Jeong BH, Um SW, Zo JI, Lee HY, Sohn I, Kim H, Kwon OJ, et al. Comparison of four models predicting the malignancy of pulmonary nodules: a single-center study of korean adults. PLoS ONE. 2018;13(7):e0201242.
42. Kammer MN, Lakhani DA, Balar AB, Antic SL, Kussrow AK, Webster RL, Mahapatra S, Barad U, Shah C, Atwater T, et al. Integrated biomarkers for the management of Indeterminate Pulmonary Nodules. Am J Respir Crit Care Med. 2021;204(11):1306–16.
43. Grogan EL, Deppen SA, Ballman KV, Andrade GM, Verdial FC, Aldrich MC, Chen CL, Decker PA, Harpole DH, Cerfolio RJ, et al. Accuracy of fluorodeoxyglucose-positron emission tomography within the clinical practice of the American College of Surgeons Oncology Group Z4031 trial to diagnose clinical stage I non-small cell lung cancer. Ann Thorac Surg. 2014;97(4):1142–8.
44. Divisi D, Barone M, Bertolaccini L, Rocco G, Solli P, Crisci R, Italian VG. Standardized uptake value and radiological density attenuation as predictive and prognostic factors in patients with solitary pulmonary nodules: our experience on 1,592 patients. J Thorac Dis. 2017;9(8):2551–9.
45. Fischer EG. Nuclear morphology and the Biology of Cancer cells. Acta Cytol. 2020;64(6):511–9.
46. Zhou J, Kulasinghe A, Bogseth A, O'Byrne K, Punyadeera C, Papautsky I. Isolation of circulating tumor cells in non-small-cell-lung-cancer patients using a multi-flow microfluidic channel. Microsyst Nanoeng. 2019;5:8.
47. Gao W, Yuan H, Jing F, Wu S, Zhou H, Mao H, Jin Q, Zhao J, Cong H, Jia C. Analysis of circulating tumor cells from lung cancer patients with multiple biomarkers using high-performance size-based microfluidic chip. Oncotarget. 2017;8(8):12917–28.
48. Miller MC, Doyle GV, Terstappen LW. Significance of circulating Tumor cells detected by the CellSearch System in patients with metastatic breast colorectal and prostate Cancer. J Oncol. 2010;2010:617421.
49. Zhang Z, Ramnath N, Nagrath S. Current status of CTCs as Liquid Biopsy in Lung Cancer and future directions. Front Oncol. 2015;5:209.
50. Habli Z, AlChamaa W, Saab R, Kadara H, Khraiche ML. Circulating Tumor Cell Detection Technologies and Clinical Utility: Challenges and Opportunities. Cancers (Basel) 2020, 12(7).
51. Rijavec E, Coco S, Genova C, Rossi G, Longo L, Grossi F. Liquid Biopsy in Non-Small Cell Lung Cancer: Highlights and Challenges. Cancers (Basel) 2019, 12(1).
52. Gil-Henn H, Patsialou A, Wang Y, Warren MS, Condeelis JS, Koleske AJ. Arg/Abl2 promotes invasion and attenuates proliferation of breast cancer in vivo. Oncogene. 2013;32(21):2622–30.
53. Shiwarski DJ, Shao C, Bill A, Kim J, Xiao D, Bertrand CA, Seethala RS, Sano D, Myers JN, Ha P, et al. To "grow" or "go": TMEM16A expression as a switch between tumor growth and metastasis in SCCHN. Clin Cancer Res. 2014;20(17):4673–88.
54. Heiden BT, Eaton DB Jr, Engelhardt KE, Chang SH, Yan Y, Patel MR, Kreisel D, Nava RG, Meyers BF, Kozower BD, et al. Analysis of delayed Surgical Treatment and oncologic outcomes in clinical stage I non-small cell Lung Cancer. JAMA Netw Open. 2021;4(5):e2111613.

Publisher's Note

Springer Nature remains neutral with regard to jurisdictional claims in published maps and institutional affiliations.